IJE TRANSACTIONS B: Applications Vol. 39, No. 05, (May 2026) 1063-1076

International Journal of Engineering

Journal Homepage: www.ije.ir

Experimental and Numerical Investigations for Improvement of Building Ventilation Performance by Using Solar Chimney Integrated with Different Phase Change Materials and Nanoparticles

W. Younus Abeid Al-Zubaidi, A. A. Ranjbar*

Faculty of Mechanical Engineering, Babol Noshirvani University of Technology, Babol, Iran

P A P E R I N F O

Paper history:
Received 26 February 2025
Received in revised form 30 June 2025
Accepted 19 July 2025

Keywords:
Natural Ventilation
Solar Chimney
Thermal Performance
Phase Change Materials

A B S T R A C T

A detailed experimental and numerical investigation of a constructed solar chimney (SC) model and its thermal performance is presented, conducted under the climatic conditions of Al-Kut City, Iraq. This study focuses on the thermal performance of two vertical solar chimneys oriented towards the south and west directions. The first configuration consists of a building with two vertical solar chimneys, incorporating two types of phase change materials (PCMs): Al-Dura paraffin wax and block-shaped paraffin wax (PCM1) and (PCM2), respectively. These PCMs are placed in the same aluminum container, separated by partitions, and equipped with fins to enhance the thermal contact area. In the second configuration, conductive mono nanoparticles (NP), specifically aluminum oxide (Al_2O_3), were introduced into both (PCM1) and (PCM2) at a volume fraction of approximately 1.6% to improve the thermal characteristics of the paraffin and overall heat storage performance. The study investigates the role of paraffin wax as an energy storage medium along with nanoparticles, where the PCM stores thermal solar energy during the day and discharges it at night through the phase change process. Numerical results demonstrate that the PCMs significantly affect air change per hour (ACH) during the day and extend ventilation hours post-sunset. The second configuration showed an ACH improvement of approximately 5.35% and a reduction in room temperature by 4.7°C compared to the first case. Experimental results indicated a 5.2% improvement in ACH and a decrease of 3.9°C in room temperature. Both experimental and numerical results confirm that integrating nanofluids with PCM significantly enhances the overall efficiency of the solar chimney. The novelty of this study lies in the innovative integration of phase change materials with conductive nanoparticles, which not only enhances the thermal performance but also significantly extends ventilation periods, especially under the high solar radiation conditions typical of AL-Kut city, Iraq. Finally, due to the intense solar radiation in AL-Kut, the passive ventilation rates achieved by the solar chimney were found to be highly satisfactory.

***doi**: 10.5829/ije.2026.39.05b.02*

Graphical Abstract

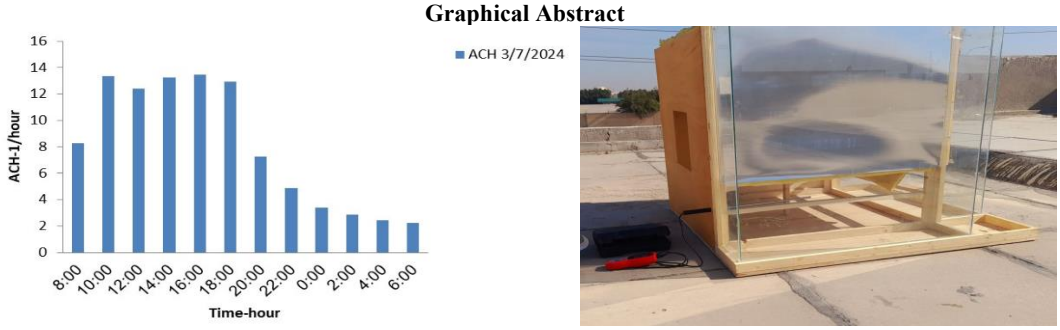

*Corresponding author email: ranjbar@nit.ac.ir (A. A. Ranjbar)

Please cite this article as: Younus Abeid Al-Zubaidi W, Ranjbar AA. Experimental and Numerical Investigations for Improvement of Building Ventilation Performance by Using Solar Chimney Integrated with Different Phase Change Materials and Nanoparticles. International Journal of Engineering, Transactions B: Applications. 2026;39(05):1063-76.

NOMENCLATURE

ACH	Air change per hour	PCM	Phase change material
Sc	Solar chimney	NP	Nanoparticles
H.F	Heat of fusion (KJ/kg)	ES	Energy storage
M.t	Melting temperature (K)	*Cp*	Specific heat (J/kg.K)
Slr	solar intensity (w/m^2)	T.room Ave	Average room temperature
k	Thermal conductivity(W/m.K)	**Greek Symbols**	
v	Viscosity (kg/m.s)	ρ	Density (kg/m^3)

1. INTRODUCTION

The solar chimney is one of the applications of negative ventilation effectiveness in providing healthy and comfortable thermal conditions, which is an air channel based on the principle of buoyancy, where the solar energy is absorbed after the energy is released to the air to create currents indoor air. The importance of the solar chimney has increased in recent years as a result of the great benefits compared to mechanical ventilation in terms of energy saving and economic cost in addition to environmental effect. The utilization of suitable energy storage is one of the options for improving the efficiency of the solar based power plants, which is as important as developing new sources of energy (1, 2). Several kinds of research and findings were conducted to study and enhance these ventilation systems arranged in this paper. Tolabi et al. (3) emphasize the importance of estimating solar radiation in solar energy systems, which requires precise and often costly equipment. The Bees Algorithm, a population-based heuristic search method implemented in MATLAB, is a new approach based on the Angstrom model. This method predicts the monthly average daily global solar radiation on a horizontal surface. The Angstrom model's experimental coefficients are calculated for Iran's six climate zones. The results demonstrate the effectiveness of this technique in providing more accurate solar radiation estimates. Ajay and Kundan (4) used a 40:60 ethylene-glycol-water mixture as the base fluid, dispersing α-Al_2O_3 nanoparticles with an average size of 20 nm to create nanofluids with four distinct volumetric concentrations (0.05%, 0.075%, 0.1%, and 0.125%). The use of nanofluid instead of a water-ethylene glycol mixture has been shown to enhance the overall efficiency of solar collectors. Bassiouny and Koura (5) employed both numerical and analytical methods to investigate the effect of vertical chimney width on space ventilation. They found that, while keeping the chimney entrance size constant, increasing the chimney width from 0.1 to 0.3 m led to a nearly 25% increase in volume flow rate. Bassiouny and Koura (6) expanded their research on inclined solar chimney performance by analyzing, both analytically and numerically, the impact of varying chimney inclination angles on indoor flow patterns and air change per hour at a latitude of 28.4°. Both analytical and numerical results showed that optimal flow rates were achieved for inclination angles between 45° and 70°. Karimipour-Fard and Beheshti (7) improved the performance of the solar chimney power plant (SCPP) by enhancing the geometrical characteristics of the collector and chimney. In the absence of solar radiation, thermal energy storage was used to generate power in the new optimal configurations. The results showed that the output power of the SCPP increased by nearly 139%, and the overall performance of the power plant improved by approximately 68.1%. Majeed and Ali (8) conducted an experimental investigation on the use of solar chimneys as heating sources in Iraqi settings. The experimental model consisted of a room with a 40° southward slope and a solar collector of specific dimensions (2.5×1.29×1.07 m). Data were collected at various points within the test area during January and February. The results showed that sun-facing walls could enhance the stored energy. Increased heat energy also promoted higher air flow rates inside the building. Jubear and Ghareer (9) used the ANSYS simulation program to perform a numerical study on how chimney inclination angles affect building ventilation. Three angles 30°, 45°, and 60° were employed, where 45° indicates the best performance. A building with two solar chimneys was later designed by the researchers. Results indicated a 31.9% improvement in ventilation efficiency and a (1.34°C) drop in temperature. Kaneko et al. (10) investigated how well solar chimneys with built-in Sulfate Dehydrate ($Na_2SO_4.10H_2O$) latent heat storage performed in terms of ventilation. According to a study done in Osaka, Japan, PCM storage inside the solar chimney was accessible for natural ventilation at night and in the evening in the event that PCM melted completely during the day. Amori and Mohammed (11) assessed the amount of energy stored and released by paraffin when added to a solar chimney, using both experimental and numerical methods. The results indicated that 5016 W of energy was stored during the 5 hour charging period, while 4954.4 W was released during the 9-hour discharging period. Imran et al. (12) conducted both experimental and numerical analyses to determine the optimal performance of a solar chimney under various geometrical conditions. Natural convection was achieved through a turbulent flux, with three air gap sizes in the solar chimney (50 mm, 100 mm, and 150 mm). The experiments were conducted at

varying angles (15°–60°) and solar radiation levels (150–750 W/m²). The results showed that the maximum ventilation rate occurred at the ideal inclination angle of 60°, with a solar radiation intensity of 750 W/m² and a 50 mm air gap. Chung et al. (13) provided the optimum values for the parameters that affect solar chimney performance. The results show that the optimum air gap is between 0.6 and 1.0 m, the chimney length is between 1.5 and 2 m, and the induced air velocity is between 0.04 and 0.22 m/s. When the air gap is 10 cm and the angle of inclination rises from 15 to 45 degrees, the ventilation rate increases by 24%. Li and Liu (14) conducted an experimental study to examine the thermal performance of a solar chimney using PCM at three different heat flux levels: 500, 600, and 700 W/m². The results showed that the PCM was completely melted only at 700 W/m², with the maximum air flow rate reaching 0.04 kg/s, and thermal efficiency exceeding 80%. This study aims to assess the thermal performance of a solar chimney and improve ventilation rates through two vertical solar chimneys. The model includes a room connected to two vertical solar chimneys, with PCM and mono nanoparticles added. The use of mechanical air cooling, especially in hot climates during the summer and sometimes in autumn and spring, extends the hours of active operation to provide optimal thermal conditions. Assari et al. (15) conducted experiments with a phase change material (PCM) triplex-tube heat exchanger, using two types of sinusoidal inner tubes: full-width and half-width. The inner, outer, and both tubes were utilized to carry out the charging and discharging processes. The results showed that the PCM melting and solidification times were shorter for the full-width sinusoidal inner tube compared to the half-width sinusoidal inner tube during both charging and discharging operations, whether from the inner tube, outer tube, or both sides. The volume and duration of PCM melting were significantly improved when comparing these processes to those of a straight inner tube. Krishna et al. (16) conducted both experimental and numerical studies to investigate the effects of using phase change material (PCM) in the adiabatic section of heat pipes for electronic cooling applications. Tricosane (100 ml) was chosen as the PCM, and Al_2O_3 nanoparticles with volume fractions of 0.5%, 1.0%, and 2.0% were dispersed throughout the PCM using an ultrasound technique. The system was tested under heating powers of 13W, 18W, and 23W. At 1.0% and 2.0% nanoparticle concentrations, the system's performance with Tricosane and nanoparticles improved and declined, respectively, suggesting an optimal nanoparticle concentration. Jadidi and Jadidi (17) highlighted that many engineering problems, such as the Stefan problem involving melting and solidification in phase change materials (PCMs), are common real-world challenges. They proposed an algorithm to solve the one-dimensional Stefan problem under various boundary conditions. Additionally, the algorithm can be easily extended to 2D and 3D Stefan problems using the finite difference approach. Kumar et al. (18) examined the literature on TiO_2 nanoparticles, specifically those that had been suspended in a 60:40 mixture of ethylene glycol and water. The results showed that the rate of heat transfer is higher when the water-ethylene glycol mixture is used at this ratio than when water is used alone. Ebrahimnataj-Tiji et al. (19) examined a PCM-enhanced solar chimney both with and without fins attached to the absorber plate. The results showed that using PCM as a storage medium improves the temperature homogeneity of the room. However, the mean of the room temperature achieved was 14.68°C, which is significantly below the thermal comfort level. Therefore, the addition of fins to the absorber was investigated to raise the room's temperature. The findings indicate that the presence of fins significantly enhances the PCM's energy storage capacity. More importantly, compared to the non-finned case, the use of fins in the PCM-based solar chimney system increases the room's mean temperature by 20%. Additionally, the finned absorber with PCM leads to more non-uniform airflow compared to the non-finned case. Selvan et al. (20) expanded motor cooling by adding two cooling channels. PCM serves as a secondary coolant, while the liquid acts as the primary coolant. Even when the liquid cooling operates at its lowest working point, this innovative cooling technique helps to maintain the bracket temperature within the permissible limit. To thoroughly examine the PCM, the main focus was on the PCM coolant channel, with the liquid coolant kept under specific working conditions. The motor cooling performance was influenced by the PCM thickness. Three different PCM channel thicknesses6 mm, 8 mm, and 10 mm were examined, with the best results observed for a PCM thickness of 6 mm, which improves heat transfer. However, aside from the articles mentioned above, similar studies conducted by other researchers can also be implicitly referred (21-26).

The goal of this study is to assess the effectiveness of natural ventilation using two solar chimneys oriented south and west, incorporating phase change materials (PCMs) as energy storage (ES) and enhancing their thermal properties with aluminum oxide (Al_2O_3) nanoparticles at a 1.6% volume fraction. The novelty of this study lies in the integration of two types of PCMs with aluminum oxide nanoparticles, which significantly enhance the thermal characteristics of paraffin wax and optimize heat storage. This approach aims to extend natural ventilation after sunset in a single-story building in the hot climate of Al-Kut, Iraq. Passive ventilation, based on the buoyancy principle, is proven effective in maintaining thermal comfort in hot climates with high

solar radiation. By using conductive nanoparticles, this study reduces reliance on active energy systems and improves overall thermal performance. The solar radiation on the system falls within the optimal range of 2000–2500 kWh/m² [1], ensuring efficiency under local conditions.

2. MODEL DESCRIPTION

The model consists of a room made of wood connected to two solar chimneys oriented in different directions (south and west). Each vertical solar chimney has dimensions of (1.0 m length, 1.0 m width, and 0.3 m depth). The solar chimneys are connected to the room through ventilation openings measuring (1.0×0.3) m² on each chimney. The room is cubical, with dimensions of (1.0×1.0×1.0) m³. The solar chimneys are made of 1.0 mm aluminum absorber panels, and 5.0 cm glass wool insulation is placed between the absorber panel and the wood to prevent heat transfer from the panel to the room. In addition, 2.5 cm of insulation is used to cover the roof of the room. The absorber panel is wrapped on three sides with a 4.0 mm-thick glass cover. The room is equipped with a window measuring (0.3×0.3) m², which is placed in the center of the northern wall to allow air to enter during the operation of the solar chimney. Figure 1 illustrates the experimental model with two vertical solar chimneys, and the schematic of the experimental setup is shown in Figure 2. The two vertical solar chimneys use two types of phase change materials (PCMs): Al-Dura paraffin wax and block-shaped paraffin wax, placed in the same aluminum container, separated by partitions. Fins are added to the PCM container to enhance heat transfer. In another case, conductive mono nanoparticles of aluminum oxide (Al_2O_3) are added to the PCMs at a volume fraction of 1.6%.

3. AIR CHANGE PER HOUR

Air change per hour (ACH) stands for Air Changes per Hour and is commonly referred to as “air exchange rate” or “air change rate”. It is a measurement of how many times a volume of air within a room will be added, removed, or exchanged with outdoor air. It was calculated according to the following equation (27):

$$ACH = \frac{3600\,A\,V}{Vr} \quad (1)$$

where A represents the area of solar chimney air entrance which equals 0.3 m², V represents the average velocity of air in the chimney entrances measured every two hours by using the hot wire anemometer, and Vr represents the volume of room that equals 1.0 m³.

4. DESCRIPTION OF ENERGY STORAGE

Two types of wax were used as an energy storage. The thermo-physical properties of the two types of wax are illustrated in the Table 1. The wax is one of the phase change materials (PCM) that charge and discharge heat during the phase change process. The dimensions of the wax container were (0.7 m in length × 0.9 m in width). Two types of PCMs namely: Al-Dura paraffin wax and Block-shaped paraffin wax.

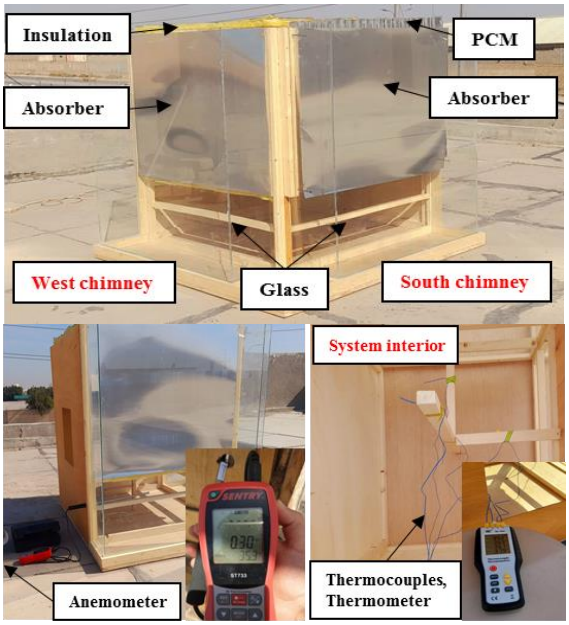

Figure 1. Experimental model with instrumnts

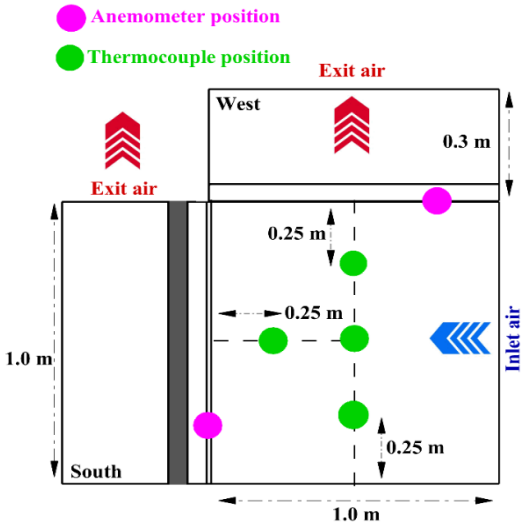

Figure 2. Schematic of experimental set up

[1] https://commons.wikimedia.org/wiki/File:483897main_GlobalPM2.5-map, https://www.pinterest.com/pin/1788070476839406962T

TABLE 1. Thermo-physical properties of wax (28, 29)

PCM	ρ	k	v	M.t	Cp	H.f
Al-Dura	786.5	0.329	0.01	326	2900	270
Block-shaped	802	0.260	0.017	329.5	2600	200
Al-Dura & Al_2O_3	836.15	0.344	0.0104	-	2737.81	250.15
Block-shaped & Al_2O_3	851.12	0.269	0.0166	-	2463.37	185.07

Thermo-physical properties of Al_2O_3 are listed in Table 2 (30, 31):

5. EXPERIMENTAL CASE STUDY

Two cases were studied over two days (3/7/2024 and 7/7/2024) in the summer climate of Al-Kut City, Iraq. In the first case, two vertical solar chimneys were used, incorporating two types of phase change materials (PCMs): Al-Dura paraffin wax and block-shaped paraffin wax, placed simultaneously in an aluminum container, separated by partitions. Fins were added to the PCM container to enhance heat transfer. The study was conducted from 8:00 AM to 6:00 PM on 3/7/2024. In the second case, conductive mono nanoparticles of aluminum oxide (Al_2O_3) were added to the PCMs at a volume fraction of 1.6% for the day of 7/7/2024, as shown in Table 3. The outcomes of the two cases were compared, and the impact of the conductive mono nanoparticles on the passive cooling system was evaluated.

5. 1. Experimental Study Procedure and Tools Measurements

The site study was conducted in Al-Kut City, Iraq, located at a longitude of (45.78E) and a latitude of (32.54N). Readings were taken every two hours, starting at 8:00 AM and finishing at 6:00 AM the following day. The measurements include solar radiation, temperature, and air velocity at the chimney air entrance. A solar power meter was used to measure the solar radiation intensity, while K-type thermocouples were employed to measure the temperatures within the building. The Sentry ST733 anemometer was used to measure air velocity at the chimney openings to calculate the air change rate (ACH) value. Tables 4 and 5 show the names, accuracy, and errors of the instruments.

TABLE 2. Thermo-physical properties of Nano-particles

Properties	ρ	k	Cp
Al_2O_3	3970	40	765

TABLE 3. Expermntal Conditions

Cases 1	3/7/2024	PCM1+ PCM2
Cases 2	7/7/2024	(PCM1+NP) + (PCM2+NP)

5. 2. Overall Uncertainty

The purpose of uncertainty calculation is to determine a confidence interval within which the true value is likely to fall. The smaller the uncertainty of the results, the higher the accuracy and precision of the parameters influencing the main data. In this section, the uncertainty of the experimental results has been calculated. According to the error distribution theory using the Taylor series, the following equation is used to calculate the uncertainty of a multivariate parameter with 95% confidence (14).

$$U_{95} = \left[\sum_{i=1}^{1} \left(\frac{\partial r}{\partial X_i}\right)^2 U_i^2\right]^{\frac{1}{2}} \quad (2)$$

Accordingly, the maximum calculation error in the graphs is 2.63%.

6. EXPERIMENTAL RESULTS AND DISCUSSIONS

In this section the experimental results are discussed. The results show that PCMs affects on ACH during the daylight period and elongates the hours of ventilation after sunset and average indoor temperature. In the first case, Table 5 depicts the thermal conditions for the day hours in Kut City, Iraq, on 3/7/2024. The peak solar intensity was 825 W/m^2 at 12:00 p.m., then progressively fell to 75 W/m^2 at 6:00 a.m. Moreover, the ambient temperature increases from 8:00 a.m. and reaches a maximum value 43 ^{o} C at 2:00 p.m. and then gradually decreases, especially in the evening and early

TABLE 4. Experimental insruments and accuracy

No.	Measuring Tools	Accuracy
1	Anemometer	±(0.03+3%)m/s
2	Solar power meter	±5 w/m^2
3	Thermocouples	±(0.1% of reading + 0.7°C)

TABLE 5. Experimental insruments and error

No.	Measuring Tools	Example	Error
1	Anemometer	measuring air velocity of 10 m/s,	±0.33 m/s
2	Solar power meter	measuring solar radiation intensity	±5% (typical)
3	Thermocouples	measuring 300°C	0.3°C + 0.7°C = ±1.0°C

morning hours reached lowest value 30 ° C at 6:00 a.m. The maximum ACH was noted around 4:00 p.m., which was equal (13.49), while the average minimum ACH was approximately (2.5) from 2:00 a.m. to 6:00 a.m. The relation between air change per hour (ACH) and test hours is illustrated in Figure 3. The experimental data shows that (ACH) begins to rise gradually after 8:00 a.m., peaks at 4:00 p.m. and drops to the lowest value from 12:00 a.m. to 6:00 a.m. due to solar intensity and sunlight orientation effects, but presences of PCMs the ventilation was continued after sunset. To specify the temperature of the building interior, three thermocouples were placed in each room at different levels. The readings were registered every two hours.

The average of the room temperatures reached the maximum values 46.4 ° C and 44.5 ° C at 2:00 p.m. and 4:00 p.m. respectively , while the minimum values were 33.5 ° C and 31.7 ° C at 4:00 a.m. and 6:00 a.m. respectively. The temperatures reading according to test periods are shown in Figure 4. The results also demonstrated that the ambient air temperature are the

TABLE 5. Experimental climate data for day (3/7/2024)

NO.	Time	T.Amb.	RH%	Slr. w/m²
1	00:00	34	15	0
2	02:00	32.6	18	0
3	04:00	31	22	0
4	06:00	30	21	75
5	08:00	34.5	17	370
6	10:00	40	14	675
7	12:00	42	12	825
8	14:00	43	11	775
9	16:00	42.4	11	520
10	18:00	41.5	12	120
11	20:00	39	13	0
12	22:00	37.6	14	0

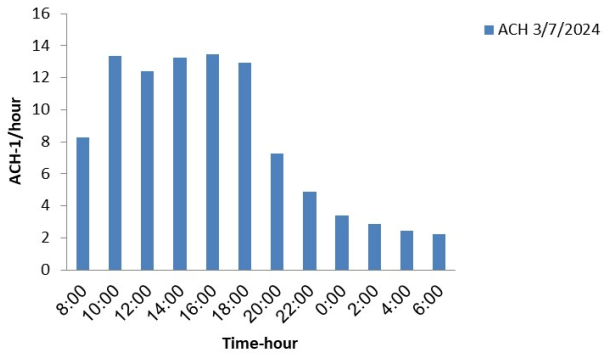

Figure 3. ACH values when using 2PCM

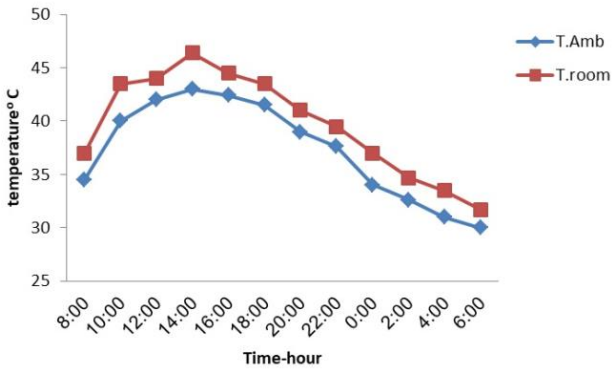

Figure 4. Room and ambient temperatures when using 2PCM

key element that affect the temperature within the building. There is a clear correlation between the temperature inside the building and the temperatures outside , the greater ambient temperature, the higher temperature inside the building.

In the second case conductive mono nanoparticles Aluminum oxide (Al_2O_3) added to Al-Dura paraffin wax & Block-shaped paraffin wax with volume fraction (1.6%). Table 6 shows the intensity of solar radiation for the day 7/7/2024, where it was the lowest value at 6:00 a.m. and amounted to 80 w/m^2, while the highest value was at noon, where it recorded 835 and 785 w/m^2 at 12:00 and 14:00, respectively, as in the sun's radiation, The highest temperature was at the afternoon hours, and it was recorded at 44 °C for 2:00 p.m., while the lowest temperature was at 6:00 a.m. and recorded at 29 °C. Table 6 also shows the average relative humidity.

The maximum ACH was noted around 4:00 p.m., which was equal (13.95) while the average minimum ACH was approximately (2.6) from 4:00 a.m. to 6:00 a.m. The ACH values are shown in Figure 5 as a

TABLE 6. Experimental climate data for day (7/7/2024)

NO.	Time	T.Amb.	RH%	Slr. w/m²
1	00:00	33	15	0
2	02:00	31	17	0
3	04:00	30.5	21	0
4	06:00	29	23	80
5	08:00	34	19	380
6	10:00	42	15	680
7	12:00	43	12	835
8	14:00	44	10	785
9	16:00	43.6	10	525
10	18:00	43	11	130
11	20:00	40.5	14	0
12	22:00	36	14	0

function of time. The results show the presences (Al_2O_3) with PCMs the ventilation was continued to 2:00 a.m. The average room temperatures reached the maximum values 46. 5 ° C and 46 ° C at 2:00 p.m. and 4:00 p.m. respectively , while the minimum values were 32 ° C and 30.5 ° C at 4:00 a.m. and 6:00 a.m. respectively. The temperatures reading according to test periods are shown in Figure 6.

6. 1. Comparison Between First and Second Experimental Cases The comparative analysis of the two experimental cases conducted on 3/7/2024 and 7/7/2024 highlights the significant improvements achieved by incorporating nanoparticle-enhanced phase change materials (2PCMs) in building thermal regulation. In the first case, conventional PCMs were utilized, and the results indicated notable effects on indoor temperature moderation and air change rates. The maximum indoor temperature reached 46.4 °C at 2:00 p.m., while the lowest was 31.7 °C at 4:00 a.m. The solar intensity peaked at 825 W/m² at noon and gradually decreased during the evening, influencing both indoor temperature and ventilation rates. The Air Changes per Hour (ACH) values demonstrated a pronounced increase after 8:00 a.m., peaking at 13.49 by 4:00 p.m., then dropping to a minimum of 2.5 during the early morning hours. In contrast, the second case incorporated mono-nanoparticles of aluminum oxide (Al_2O_3) into paraffin wax at a concentration of 1.6%. This modification led to a more favorable thermal environment. The maximum room temperature was slightly lower at 44 °C, and the minimum was 29 °C, suggesting better thermal control. Despite a slightly higher solar radiation intensity, reaching 835 W/m² at noon, the 2PCM with (Al_2O_3) system managed to stabilize indoor conditions more effectively than the traditional PCM setup. Importantly, the second case displayed a more uniform and sustained ventilation pattern. The ACH values followed a similar trend to the first case but exhibited a smoother distribution, indicating less thermal stress and more consistent air exchange throughout the day. This implies enhanced indoor air quality and prolonged natural ventilation effectiveness, even during hours when solar radiation diminished. The improved thermal conductivity provided by the nanoparticles allowed the 2PCM material to absorb and release heat more efficiently, thereby reducing peak indoor temperatures and extending the cooling effect beyond sunset.This suggests strong potential for implementing nanoparticle-enhanced PCMs in sustainable building applications, especially in hot climates where thermal regulation is critical.

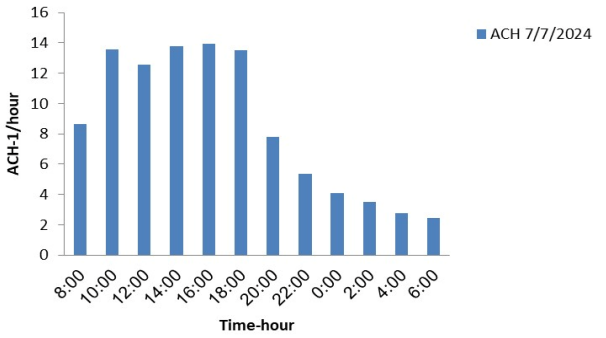

Figure 5. ACH values when using 2 PCM & NP volume fraction 1.6%

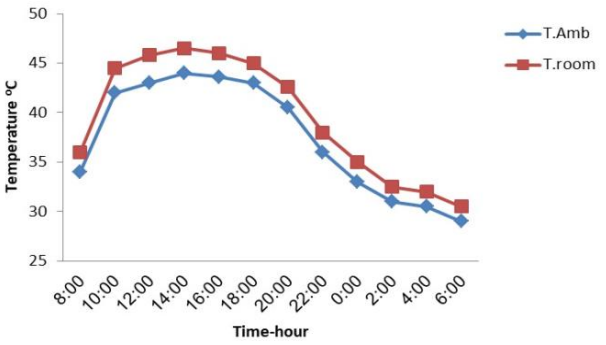

Figure 6. Room and ambient temperatures when using 2 PCM & NP volume fraction 1.6%

7. NUMERICAL SIMULATION

CFD analysis of the absorber tube of the solar chimney is done through ANSYS FLUENT 2022 R1. To obtain the optimal solution for implementing the numerical simulation in the ANSYS Fluent program, the following steps are followed:

- Create the numerical models using SolidWorks.
- Configure the numerical model in ANSYS Fluent and create a mesh appropriate for the model, ensuring that the software functions correctly.
- Select the appropriate solution by activating the energy equations, the turbulent flow (K-epsilon) model, and the radiation equation.
- Introduce the properties of the following materials: Air, Glass, Wood, Absorber panel (Aluminum), Insulation materials and Phase change materials.
- Define the boundary conditions of the model, which include ambient temperature, atmospheric pressure, and solar radiation, as well as the emissivity, absorptivity, and reflectivity of the materials.
- Initialize the flow procedure.
- Run the simulation and perform calculations.
- Save the results.

7. 1. Boundary Conditions Figure 7a-b shows the room connected to the solar chimney consists of

cubical wooden with dimensions (1×1×1) m^3 and the roof was covered with insulation. All walls of the model are opaque, except in the solar chimney has three semi-transparent wall made of glass. The solar chimney consisted from channel has a glass facade is used to allow the solar radiation to penetrate the glass surface of chimney to heat the aluminum absorber panel. In both cases of CFD simulation the type of boundary at the inlet and outlet of the model are pressure inlet and pressure outlet (atmospheric pressure) and no-slip condition between the fluid and wall. A standard k-ε model of turbulent flow was associated with the laws of the wall along solid boundaries is employed, where are depended on the Rayleigh number (Ra) > 10^8 and type of turbulent flow. Rayleigh number is a dimensionless number used in fluid dynamics and heat transfer to determine the occurrence of convection or buoyancy-driven flow in a fluid system. The solar radiation was simulated by the Discrete Ordinates (DO) model. The simple algorithm is use for coupling of continuity and pressure. The walls are non-adiabatic heat transfer by conduction, convection and radiation consideration.

7. 2. MESH Independence Figure 7c shows the computational mesh. To examine the computational mesh resolution, five different meshes were created for the 3D model of the solar chimney, and the simulation was performed using ANSYS Fluent software, as shown

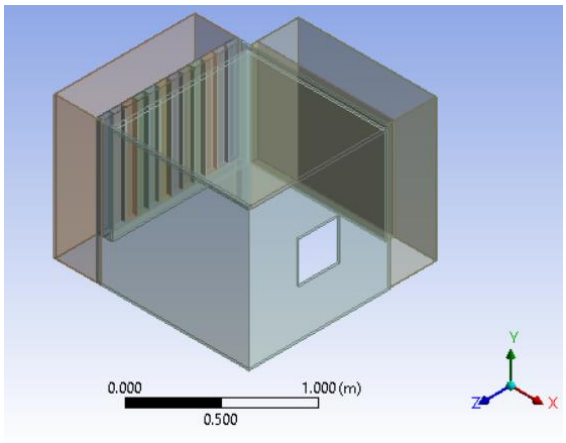

(a) Two vertical solar chimneys

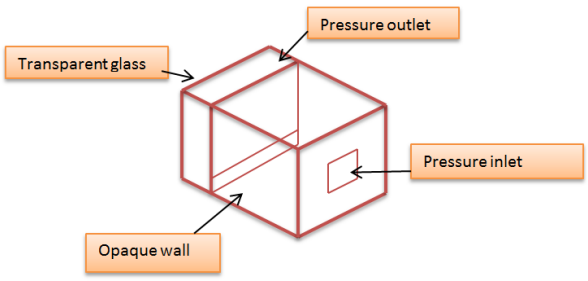

(b) Boundary condition of model

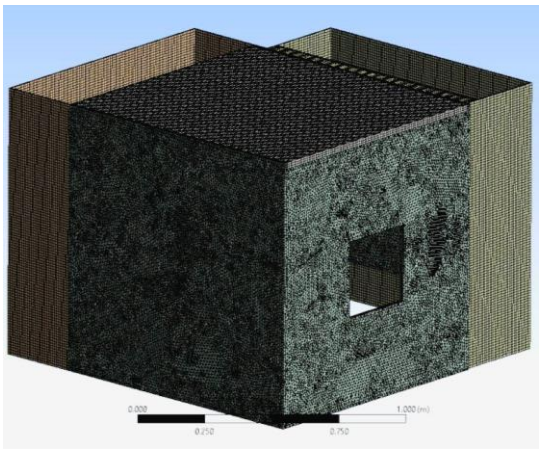

(c) The computational mesh.

Figure 7. Experimental solar chimney studied model

in Table 7. Based on the CFD simulation results of the ventilation system, two parameters—room temperature and air changes per hour (ACH)—were considered to assess the mesh accuracy.The optimum mesh selected is (9929188) elements in model 4, through which can reach accurate results and short time in solution.

8. NUMERICAL RESULTS AND DISCUSSIONS

In this section we will discuss the numerical results on 3/7/2024 and analysis the numerical results of thermal performance of solar chimney ventilation (ACH, room average temperature, and hours of ventilation). The maximum ACH was noted around 4:00 p.m., which was equal (14.1), while the minimum ACH was approximately (2.8) from 2:00 a.m. to 6:00 a.m. The ACH values are shown in Figure 8 as a function of time. The average room temperatures reached the maximum values 45.2 ° C and 44 ° C at 2:00 p.m. and 4:00 p.m. respectively , while the minimum values were 33 ° C and 31 ° C at 4:00 a.m. and 6:00 a.m. respectively.

The temperatures reading according to test periods are in Figure 9. The ventilation took place between 8:00 a.m. and 12:00 a.m. on the next day depending on the values of the ACH, which change during these hours and then approximately stabilize at fixed values after

TABLE 7. Choosing the optimum mesh

No.	Elements	Nodes	Total ACH	Total T.Ave.Room
1	4378215	932559.795	81.6	471.2
2	7390644	1574207.172	92.73	471.6
3	8376886	1784276.718	95.46	470.87
4	9929188	2114917.044	96.82	470.54
5	12582098	2679986.874	97.79	471.13

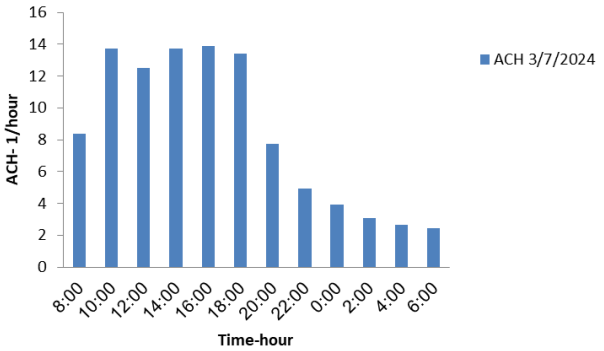

Figure 8. ACH values when using 2PCM

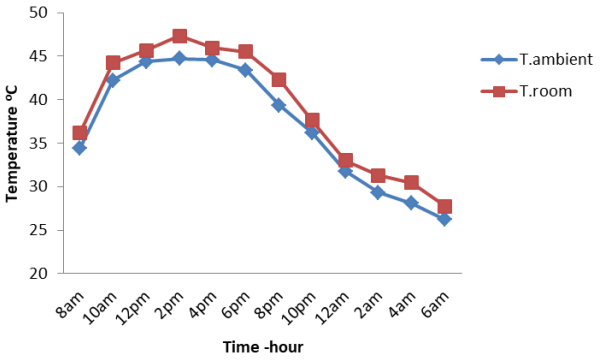

Figure 9. Room and ambient temperatures when using 2 PCM

12:00 a.m. To demonstrate the behavior of air velocity and temperature in this case through the day when using these two types of wax, Figures 10 and 11 illustrate the velocity and temperature contours at 12:00 p.m.

The process of melting and solidification of wax had an impact on the ventilation rate because the temperature of the wax affects the temperature of the absorbent wall. Figures 12 and 13 illustrate the liquid fraction at 12:00 p.m. and 12:00 a.m., respectively.

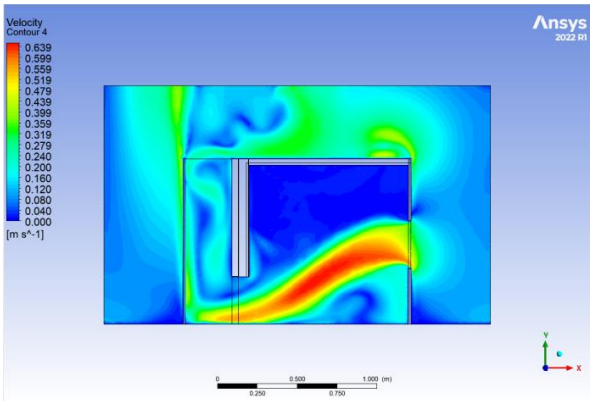

Figure 10. Velocity distribution when using 2PCM at 12:00 p.m.

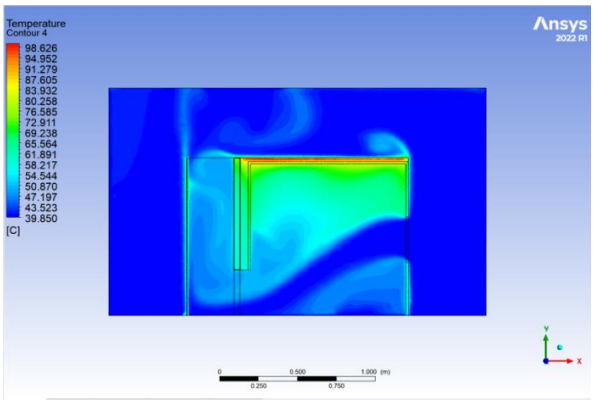

Figure 11. Temperature distribution when using 2PCM at 12:00 p.m.

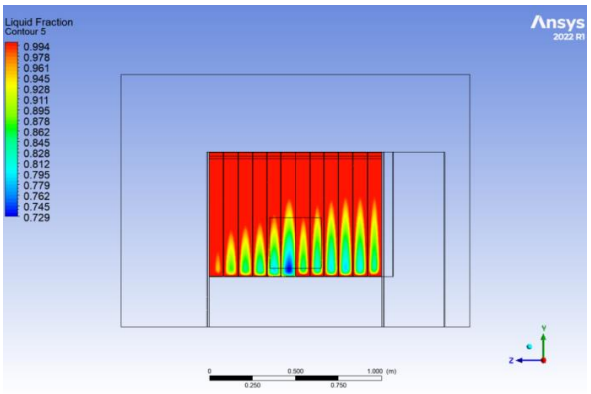

Figure 12. Liquid fraction when using 2PCM at 12:00 p.m.

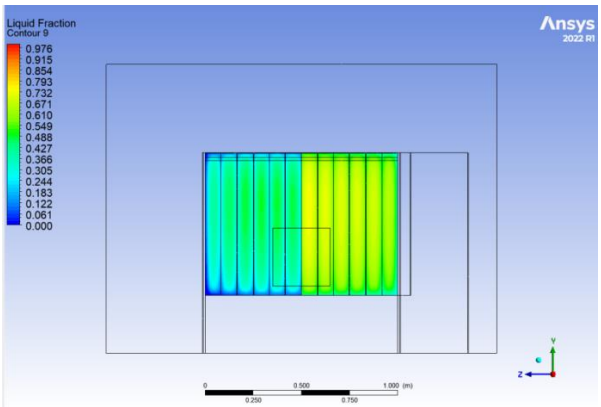

Figure 13. Liquid fraction when using 2PCM at 12:00 a.m.

Second case was on 7/7/2024 , the results showed that the best case added conductive mono nanoparticles Aluminum oxide to Al-Dura paraffin wax & Block-shaped paraffin wax with volume fraction (1.6%). The maximum ACH was noted around 4:00 p.m., which was equal (14.3) while the minimum ACH was approximately (2.9) from 4:00 a.m. to 6:00 a.m. The ACH values are shown in Figure 14 as a function of

time. The average room temperatures reached the maximum values 45 ° C and 44.7 ° C at 2:00 p.m. and 4:00 p.m. respectively , while the minimum values were 30.26 °C and 27.23 ° C at 4:00 a.m. and 6:00 a.m. respectively. The temperatures reading according to test periods are in Figure 15.

The ventilation took place between 8:00 a.m. and 2:00 a.m. on the next day depending on the values of the ACH, which changed during these hours and then approximately stabilized at fixed values after 2:00 a.m. To demonstrate the behavior of air velocity and temperature in this case through the day when using these two types of wax and NP volume fraction 1.6% , Figures 16 and 17 illustrate the velocity and temperature contours at 12:00 p.m.

The process of melting and solidification of wax had an impact on the ventilation rate because the temperature of the wax affects the temperature of the absorbent wall which affects the temperature of the air adjacent to the absorber wall. Figures 18 and 19 illustrate the liquid fraction at 12:00 p.m. and 12:00 a.m., respectively.

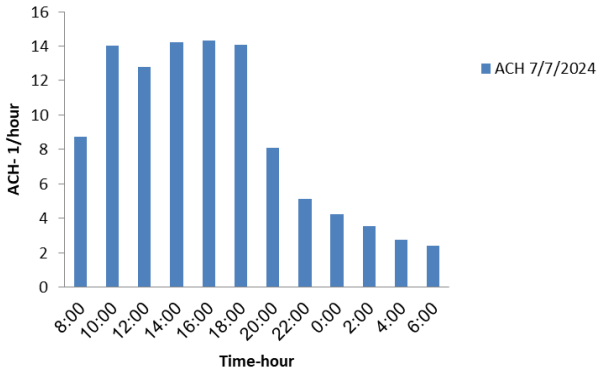

Figure 14. ACH values when using 2 PCM & NP volume fraction 1.6%

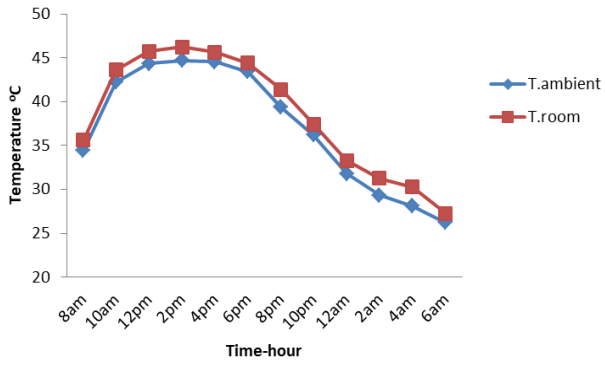

Figure 15. T.room and T. ambient when using 2 PCM & NP volume fraction 1.6%

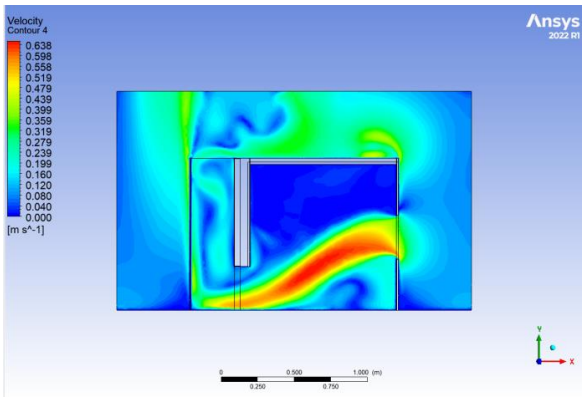

Figure 16. cVelocity distribution when using 2 PCM & NP volume fraction 1.6% at 12:00 p.m.

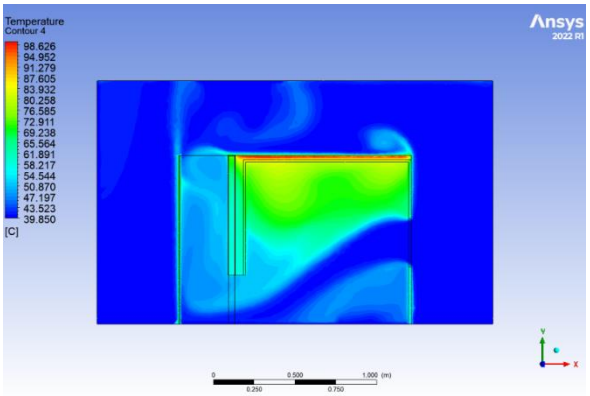

Figure 17. Temperature distribution when using 2 PCM & NP volume fraction 1.6% at 12:00 p.m.

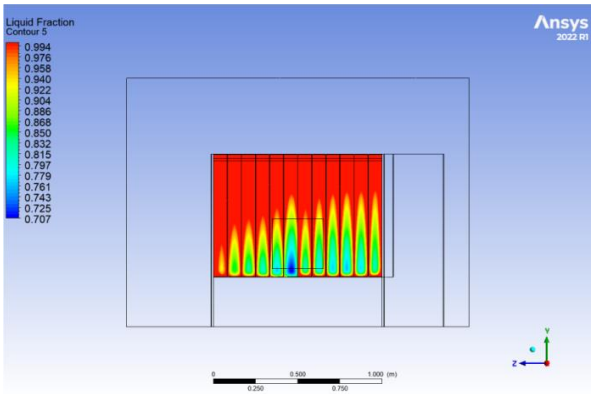

Figure 18. Liquid fraction when using 2 PCM & NP volume fraction 1.6% at 12:00 p.m.

8. 1. Comparison between First and Second Numerical Cases The numerical simulations conducted for both experimental cases offer critical insights into the thermal behavior, ventilation efficiency, and dynamic responses of the solar chimney-integrated systems under varying PCM configurations.

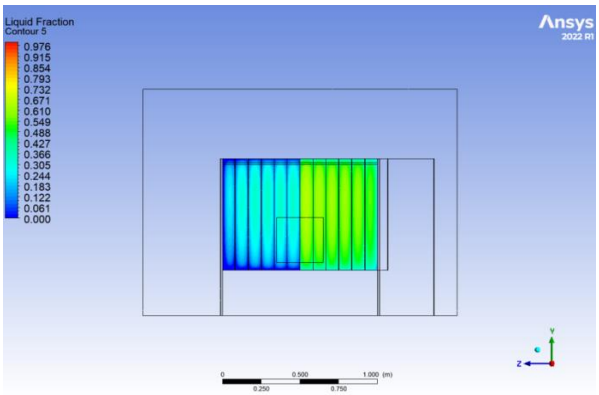

Figure 19. Liquid fraction when using 2 PCM & NP volume fraction 1.6% at 2:00 a.m.

In the first case (3/7/2024), which employed standard PCMs, the maximum ACH (Air Changes per Hour) reached 14.1 at 4:00 p.m., while the minimum dropped to 2.8 during the early morning hours (2:00–6:00 a.m.). The room temperature peaked at 46.4 °C at 2:00 p.m. and 4:00 p.m., and decreased to 33 °C and 31 °C at 4:00 a.m. and 6:00 a.m., respectively. The ventilation period extended from 8:00 a.m. to 12:00 a.m., based on ACH values, and showed a distinct correlation with solar radiation and ambient temperature fluctuations. Conversely, the second case (7/7/2024) incorporated 2PCMs enhanced with 1.6% aluminum oxide (Al_2O_3) nanoparticles, and the simulation demonstrated notable improvements in performance. The maximum ACH slightly increased to 14.3, with a more consistent and sustained ventilation pattern lasting from 8:00 a.m. to 2:00 a.m. The room temperature fluctuated between 27.23 °C and 44.7 °C, significantly lower than in the first case, especially during nighttime, confirming enhanced thermal regulation. This can be attributed to the improved thermal conductivity of the nano-enhanced PCM, which allows for faster and more effective heat absorption and dissipation. Visual analyses, including Figures 10 through 17, further validated these findings. The velocity and temperature distributions revealed stronger and more uniform airflow patterns in the second case, particularly around the absorber and exit zones of the solar chimney. The liquid fraction contours at 12:00 p.m. (Figure 12) and 12:00 a.m. (Figure 13) confirmed superior melting characteristics in the second case, with a wider and more active heat transfer zone. These improvements positively impacted the buoyancy-driven airflow, supporting higher ACH values and more effective cooling.

8. 2. Comparison between Numerical and Experimental Results A comparison between the numerical and experimental results reveals a close agreement in both air changes per hour (ACH) and average room temperature, with minor deviations attributed to physical factors such as heat losses from the solar chimney and the influence of wind speed. In the first case (3/7/2024), the experimental results showed a maximum ACH of 13.49 at 4:00 p.m., while the numerical simulation predicted a slightly higher value of 14.1 at the same time. The average deviation in ACH between the experimental and numerical results was calculated at 6.6%. Regarding the temperature, the experimental measurements recorded the maximum room temperatures of 46.4°C and 44.5°C at 2:00 p.m. and 4:00 p.m. respectively, while the numerical results showed corresponding values of 45.2°C and 44°C. The deviation in average room temperature between the two methods was 2.1%,as illustrated in Figures 20 and 22. In the second case (7/7/2024), where conductive mono nanoparticles (Al_2O_3) were added to the paraffin wax, the experimental ACH peaked at 14.3 at 4:00 p.m., while the numerical model reported a deviation of 5.9%. The experimental maximum room temperatures reached 45°C and 44.7°C at peak times, with minimum values of 30.26°C and 27.23°C recorded during early morning hours. The average temperature deviation between numerical and experimental results in this case was 3.1%,as seen in Figures 21 and 23. These results

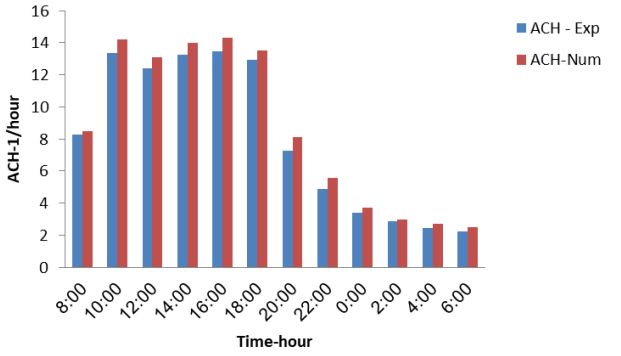

Figure 20. Comparison ACH for experimental and numerical results of case 1

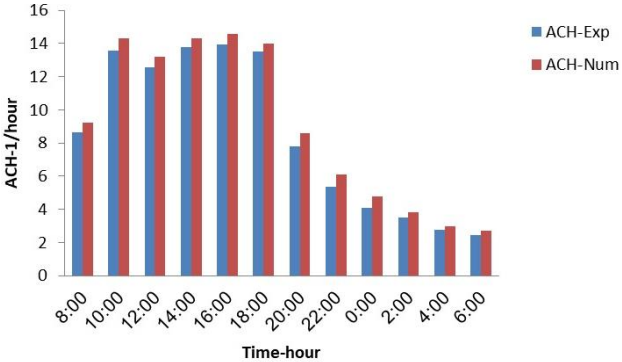

Figure 21. Comparison ACH for experimental and numerical results of case 2

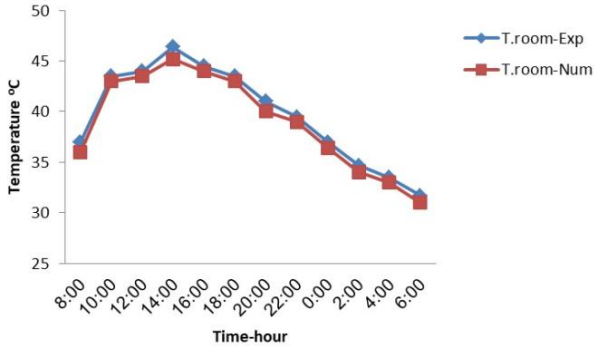

Figure 22. Comparison T.room for experimental and numerical results of case 1

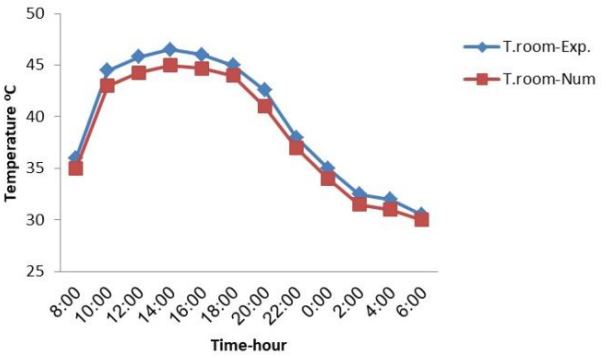

Figure 23. Comparison T.room for experimental and numerical results of case 2

confirm the reliability of the numerical model, as it successfully captured the trends and performance of the experimental setup with reasonable accuracy. The small discrepancies can be attributed to environmental conditions and assumptions within the simulation model.

9. CONCLUSIONS

This study presents a comprehensive investigation of the thermal performance of solar chimney systems integrated with phase change materials (PCMs) and nanoparticle-enhanced phase change materials under the climatic conditions of Al-Kut City, Iraq. The results from both experimental and numerical simulations show that combining conductive nanoparticles, such as aluminum oxide (Al_2O_3), with PCM-based paraffin significantly improves the thermal performance and ventilation of solar chimney systems. The key findings are as follows:

- The incorporation of PCMs significantly increases the air changes per hour (ACH) during daylight hours and extends ventilation time after sunset. Specifically, in the second configuration, which utilized nanoparticle-enhanced PCMs, there was an improvement in ACH by approximately 5.35% and a reduction in room temperature by 4.7°C compared to the first configuration. This highlights the effective role of PCMs in regulating indoor temperature and maintaining airflow after sunset.
- The addition of 1.6% aluminum oxide nanoparticles to paraffin wax improved heat absorption and release properties, resulting in a more uniform and continuous ventilation pattern. This change led to a slight increase in the maximum ACH from 14.1 to 14.3 and a reduction in internal temperature fluctuations, which were clearly reduced throughout the day and night.
- In the second configuration, which used nanoparticle-enhanced PCMs, better thermal regulation was observed. The maximum room temperature decreased by 2.4°C, and indoor temperatures during the night were significantly lower, enhancing the comfort of the indoor environment.
- The numerical simulations closely matched the experimental results, with a slight deviation of 6.6% for ACH and 2.1% for room temperature in the first case, and 5.9% for ACH and 3.1% for room temperature in the second case. This indicates the reliability of the numerical model in predicting the performance of solar chimney systems with various configurations.
- The results of this study indicate the potential of using nanoparticle-enhanced PCMs to improve the performance of passive solar ventilation systems, especially in hot regions such as Al-Kut. This innovation not only enhances the thermal performance of solar chimneys but also contributes to energy savings and improved indoor air quality, ultimately promoting sustainable building practices.

Future research should explore the long-term impacts of these systems under various climatic conditions, as well as the scalability of these systems for larger buildings and urban applications, expanding the use of these advanced materials as a crucial step in developing sustainable building technologies.

10. REFERENCES

1. Rezaie B, Reddy BV, Rosen MA. Exergy analysis of thermal energy storage in a district energy application. Renewable Energy. 2015;74:848-54. https://doi.org/10.1016/j.renene.2014.09.014
2. Sadafi M, Hosseini R, Safikhani H, Bagheri A, Mahmoodabadi M. Multi-objective optimization of solar thermal energy storage using hybrid of particle swarm optimization and multiple crossover and mutation operator. International Journal of Engineering Transactions B: Applications. 2011;24:366-76. https://doi.org/10.5829/idosi.ije.2011.24.04b.07

3. BAGHERI TH, Moradi M, BAGHERI TF. New technique for global solar radiation forecast using bees algorithm. International Journal of Engineering Transactions B: Applications. 2013;26:1385-92. https://doi.org/10.5829/idosi.ije.2013.26.11b.14
4. Ajay K, Kundan L. Performance evaluation of nanofluid (al2o3/h2o-c2h6o2) based parabolic solar collector using both experimental and cfd techniques. International Journal of Engineering-Transactions A: Basics. 2016;29(4):572-80. https://doi.org/10.5829/idosi.ije.2016.29.04a.17
5. Bassiouny R, Koura NS. An analytical and numerical study of solar chimney use for room natural ventilation. Energy and buildings. 2008;40(5):865-73. https://doi.org/10.1016/j.enbuild.2007.06.005
6. Bassiouny R, Korah NS. Effect of solar chimney inclination angle on space flow pattern and ventilation rate. Energy and Buildings. 2009;41(2):190-6. https://doi.org/10.1016/j.enbuild.2008.08.009
7. Karimipour-Fard P, Beheshti H. Performance enhancement and environmental impact analysis of a solar chimney power plant: Twenty-four-hour simulation in climate condition of isfahan province, iran. International Journal of Engineering Transactions B: Applications. 2017;30(8):1260-9. https://doi.org/10.5829/ije.2017.30.08b.20
8. Majeed MH, Ali A. Passive solar heating of a space. IOSR Journal of Mechanical and Civil Engineering. 2016;13(6):101-7. https://doi.org/10.9790/1684-130605101107
9. Jubear AJ, Ghareer AD. Numerical investigations on solar chimney inclination angle for room ventilation. International Journal of Engineering & Technology. 2018;7(4.17):1-9.
10. Kaneko Y, Sagara K, Yamanaka T, Kotani H, Sharma S, editors. Ventilation performance of solar chimney with built-in latent heat storage. Proceedings of 10th international conference of thermal energy conference (ECOSTOCK); 2006.
11. Amori KE, Mohammed SW. Experimental and numerical studies of solar chimney for natural ventilation in Iraq. Energy and Buildings. 2012;47:450-7. https://doi.org/10.1016/j.enbuild.2011.12.014
12. Imran AA, Jalil JM, Ahmed ST. Induced flow for ventilation and cooling by a solar chimney. Renewable energy. 2015;78:236-44. https://doi.org/10.1016/j.renene.2015.01.019
13. Chung LP, Ahmad MH, Ossen DR, Hamid M. Effective solar chimney cross section ventilation performance in Malaysia terraced house. Procedia-Social and Behavioral Sciences. 2015;179:276-89. https://doi.org/10.1016/j.sbspro.2015.02.431
14. Li Y, Liu S. Experimental study on thermal performance of a solar chimney combined with PCM. Applied Energy. 2014;114:172-8. https://doi.org/10.1016/j.apenergy.2013.09.022
15. Assari M, Basirat Tabrizi H, Parvar M, Alkasir Farhani M. Experimental investigation of sinusoidal tube in triplex-tube heat exchanger during charging and discharging processes using phase change materials. International Journal of Engineering Transactions A: Basics, . 2019;32(7):999-1009. https://doi.org/10.5829/IJE.2019.32.07A.13
16. Krishna J, Kishorea P, Solomonb AB, Sharmac VK. Experimental and Numerical Investigations on Al2O3–Tricosane Based Heat Pipe Thermal Energy Storage. International Journal of Engineering Transactions C: Aspects. 2018;31:980-5. https://doi.org/10.5829/IJE.2018.31.06C.16
17. Jadidi A, Jadidi M. An algorithm based on predicting the interface in phase change materials. International Journal of Engineering Transactions B: Applications. 2018;31(5):799-804. https://doi.org/10.5829/ije.2018.31.05b.15
18. Vandrangi S, Hassan S, Sharma K, Baheta A. Heat Transfer Coefficients Investigation for TiO2 Based Nanofluids. International Journal of Engineering, Transactions A: Basics. 2019;32:1491-6. https://doi.org/10.5829/ije.2019.32.10a.19
19. Tiji ME, Eisapour M, Yousefzadeh R, Azadian M, Talebizadehsardari P. A numerical study of a PCM-based passive solar chimney with a finned absorber. Journal of Building Engineering. 2020;32:101516. https://doi.org/10.1016/j.jobe.2020.101516
20. Selvana J, Manavalla S. An Innovative and Reliable Hybrid Cooling Method for Electric Vehicle Motors. International Journal of Engineering Transactions A: Basics 2024;37(07):1263. https://doi.org/10.5829/IJE.2024.37.07A.06
21. Ali MH, Mawlood MK, Jalal RE. Investigation of the performance of a newly designed solar chimney for enhancing natural ventilation and mitigation of summer overheating. Journal of Building Engineering. 2024;95:110310. https://doi.org/10.1016/j.jobe.2024.110310
22. Huang S, Li W, Lu J, Li Y, Wang Z, Zhu S. Experimental study on thermal performances of a solar chimney with and without PCM under different system inclination angles. Energy. 2024;290:130154. https://doi.org/10.1016/j.energy.2023.130154
23. Saleh MJ, Ahmed OK, Atallah FS. Comparison assessment for the effect of porous media and phase change material on the performance of photovoltaic solar chimney. Journal of Energy Storage. 2024;98:113158. https://doi.org/10.1016/j.est.2024.113158
24. Nia ES, Ghazikhani M. Enhancing reliability and efficiency of solar chimney by phase change material Integration: An Experimental study. Thermal Science and Engineering Progress. 2024;51:102600. https://doi.org/10.1016/j.tsep.2024.102600
25. Sornek K, Figaj R, Papis-Frączek K. Development and tests of the novel configuration of the solar chimney with sensible heat storage. Applied Thermal Engineering. 2025;258:124515. https://doi.org/10.1016/j.applthermaleng.2024.124515
26. Hassan HZ. Performance enhancement of the basic solar chimney power plant integrated with an adsorption cooling system with heat recovery from the condenser. Energies. 2023;17(1):136. https://doi.org/10.3390/en17010136
27. Qasim HH, Alshara AK, Abood FA. Simulation and design of a solar chimney integrated with phase change material layer for building ventilation. International Journal of Thermofluids. 2024;24:100853. https://doi.org/10.1016/j.ijft.2024.100853
28. ALubaidi AB, Abas FO, Abass RA, Abdulredhi NJ. Thermal Behaviour of Paraffin Wax/Poly Vinyl Alcohol Composite Material. Al-Khwarizmi Engineering Journal. 2016;12(2):18-26.
29. Li C, Li Q, Ge R. Fabrication and investigation of paraffin based shape-stable composite phase change materials with styrene ethylene butylene styrene as supporting skeleton for low temperature thermal energy storage and management. Journal of Energy Storage. 2023;68:107802. https://doi.org/10.1016/j.est.2023.107802
30. Alawi OA, Sidik NAC, Xian HW, Kean TH, Kazi SN. Thermal conductivity and viscosity models of metallic oxides nanofluids. International Journal of Heat and Mass Transfer. 2018;116:1314-25. https://doi.org/10.1016/j.ijheatmasstransfer.2017.09.133
31. Daood IY. Effects of nano-fluids types, volume fraction of nano-particles, and aspect ratios on natural convection heat transfer in right-angle triangular enclosure. Eng And Tech Journal. 2010;28(16):5365-88.

Persian Abstract

چکیده

یک تحقیق تجربی و عددی دقیق از مدل ساخته شده دودکش خورشیدی (SC) و عملکرد حرارتی آن ارائه شده است که تحت شرایط اقلیمی شهر ال-کوت، عراق انجام شده است. این مطالعه بر روی عملکرد حرارتی دو دودکش خورشیدی عمودی با جهت‌گیری به سمت جنوب و غرب تمرکز دارد. پیکربندی اول شامل یک ساختمان با دو دودکش خورشیدی عمودی است که دو نوع ماده تغییر فاز (PCM) را در بر می‌گیرد: واکس پارافین آل-دورا و واکس پارافین بلوک‌شکل (PCM1) و (PCM2)، به ترتیب. این مواد PCM در همان ظرف آلومینیومی قرار داده شده‌اند، که توسط partitions از یکدیگر جدا شده‌اند و با فین‌ها تجهیز شده‌اند تا سطح تماس حرارتی را افزایش دهند. در پیکربندی دوم، نانوذرات تک‌عنصری (NP)، به‌ویژه اکسید آلومینیوم (Al_2O_3)، به هر دو ماده PCM1 و PCM2 در یک حجم تقریبی ۱/۶٪ اضافه شده‌اند تا ویژگی‌های حرارتی پارافین و عملکرد ذخیره‌سازی گرما را بهبود بخشند. این مطالعه نقش واکس پارافین را به‌عنوان یک ماده ذخیره‌سازی انرژی همراه با نانوذرات بررسی می‌کند، به‌طوری که PCM انرژی خورشیدی حرارتی را در طول روز ذخیره کرده و در شب از طریق فرآیند تغییر فاز آن را آزاد می‌کند. نتایج عددی نشان می‌دهند که مواد PCM تأثیر قابل توجهی بر میزان تغییر هوای در ساعت (ACH) در طول روز دارند و ساعات تهویه پس از غروب آفتاب را تمدید می‌کنند. پیکربندی دوم نشان داد که ACH حدود ۵/۳۵٪ بهبود یافته و دمای اتاق به میزان ۴/۷ درجه سانتی‌گراد کاهش یافته است در مقایسه با مورد اول. نتایج تجربی نشان داد که ACH به میزان ۵.۲٪ بهبود یافته و دمای اتاق ۳/۹ درجه سانتی‌گراد کاهش یافته است. نتایج تجربی و عددی هر دو تأیید می‌کنند که ادغام نانو سیالات با PCM به طور قابل توجهی کارآیی کلی دودکش خورشیدی را بهبود می‌بخشد. نوآوری این مطالعه در ادغام نوآورانه مواد تغییر فاز با نانوذرات هدایت‌کننده است که نه تنها عملکرد حرارتی را بهبود می‌بخشد بلکه به‌طور چشمگیری دوره‌های تهویه را تمدید می‌کند، به‌ویژه تحت شرایط تابش خورشیدی شدید که در شهر ال-کوت، عراق معمول است. در نهایت، به‌دلیل تابش خورشیدی شدید در ال-کوت، نرخ‌های تهویه غیرفعال که توسط دودکش خورشیدی به‌دست آمد، بسیار رضایت‌بخش گزارش شد.